International Journal of Applied Power Engineering (IJAPE)
Vol. 14, No. 4, December 2025, pp. 893~902
ISSN: 2252-8792, DOI: 10.11591/ijape.v14.i4.pp893-902

PD characteristics of polymer insulation for inverted-fed drives under sine and square waveforms

S. Narasimha Rao[1], Elanseralathan Kasinathan[2], Ramanujam Sarathi[3]
[1]Department of Electrical and Electronics Engineering, Siddharth Institute of Engineering & Technology, Puttur, India
[2]Department of Electrical and Electronics Engineering, Puducherry Technological University, Puducherry, India
[3]Department of Electrical Engineering, Indian Institute of Technology Madras, Chennai, India

Article Info

Article history:

Received Nov 21, 2023
Revised Aug 28, 2025
Accepted Oct 16, 2025

Keywords:

Electric field distribution
High switching frequency
Modeling
PRPD
Square wave voltage
Twisted pair

ABSTRACT

In recent years, adjustable speed drives power by power electronic converters have caused insulation failure in the electrical motors with stator windings. The repeating impulse voltages produced by IGBTs created insulation reliability problems in the stator winding. Overvoltage can cause partial discharge (PD), which can rapidly result in insulation system failure. To address this issue, IEC standards and technical specifications (TS) necessitate that a PD test on the motor insulation system is done at sinusoidal and square voltages. The PD characteristics obtained are used to evaluate insulation performance, enhancing insulation design. This work focuses on the PD characterization of twisted pair samples using high frequency sine and square waveforms at room temperature. The PD characteristics were investigated at 50 Hz, 1 kHz, 2.4 kHz, and 5 kHz. The result shows that there are fewer PD events with lower PD magnitudes and shorter delay times at higher frequencies. Further, at different temperatures of 30 °C, 60 °C, and 90 °C, the partial discharge inception voltage (PDIV) of twisted pair insulation was investigated using high-frequency sine and square waveforms. The results show that the corona inception voltage (CIV) (kV) decreases as ambient temperature increases. Furthermore, the conditions for PD occurrence in the insulation system were analyzed at higher switching frequencies. The electric field distribution of twisted pairs with a 0 mm air gap was modeled from 50 Hz to 5 kHz switching frequency using COMSOL software.

Corresponding Author:

S. Narasimha Rao
Department of Electrical and Electronics Engineering, Siddharth Institute of Engineering & Technology
Puttur, Andhra Pradesh 517583, India
Email: snrinskit@ptuniv.edu.in

1. INTRODUCTION

Inverter-fed motors are now widely employed in numerous industries, including high-speed railroads, hybrid electrical vehicles (HEVs), and many industrial applications, due to several advantages such as high efficiency and controllability [1]. Unlike conventional motors powered by sinusoidal AC supply, modern inverter-fed motors utilize pulse width modulation (PWM) techniques, characterized by high-frequency, fast-rising voltage pulses generated by advanced switching devices such as IGBTs [2]. As a result, the coil's enamel insulation experiences frequent surge voltages with nanosecond rise times. Low and medium voltage motors are both affected by these surges, which cause reliability issues [3]. Additionally, excess voltages may build up at the phase-to-phase and turn-to-turn insulation terminals of the motor winding, up to twice the input voltage, as a result of reflection, resonance effects, and impedance mismatches between the inverter, cable, and motor [4], [5]. The unexpected early breakdown of motor winding insulation is caused by these forces [6], [7].

Additionally, there is an uneven distribution of electrical potential across the windings. This leads to greater electrical stress on phase-to-ground and turn-to-turn insulation than that caused by a sinusoidal waveform [8], especially in the early turns [9]. High switching frequency can cause overvoltage and the start of partial discharge (PD) activity when there are fast rising/falling voltages present. This causes the organic insulating materials used in winding insulation to degrade rapidly [10], [11]. As a result, the International Electro technical Committee (IEC) has produced IEC TS 60034-18-41 and IEC TS 60034-18-42 to improve the insulating reliabilities of inverter-fed motors [12], [13]. IEC standards have been addressed individually for examining the adverse effects of PD on inverter-fed motor insulation systems, according to the technical specifications (TS). PD is prohibited throughout the whole lifespan of random-wound motors (type I, rated voltage < 700 V). As a result, during qualification and acceptance tests, the partial discharge inception voltage (PDIV) should be identified to ensure that it is adequate to prevent PD during the motor's expected lifetime [12].

A study of low-frequency PDIV behavior on type I enamel insulation has been reported [14]. However, when employed in speed control applications, enamel insulation is subjected to higher frequency stresses, significantly degrading the motor winding insulation [15]. This work shows the PDIV at different temperatures of 30 °C, 60 °C, and 90 °C, at various frequency levels ranging from 50 Hz to 5 kHz, as well as the PD characteristics of square and sine waveforms at various frequency levels ranging from 50 Hz to 5 kHz at room temperature. The IEC TS 60034-18-41 standard [16] has a significant impact on rotating machine evaluation and performance. According to the above-mentioned document, square wave voltage is used to assess PDIV for type-I insulation systems that produce the highest dv/dt, which may create dielectric and thermal stresses on the insulation system when compared to a sine waveform. The growing number of low voltage motors and the increased demand for variable-speed electrical machine applications are the reasons for choosing a high frequency [17], [18]. In order to examine the electric stress caused by rapidly increasing high-frequency voltage pulses on motor winding insulation as a result of IGBT operation, high-frequency switching is used in this work and to investigate the differences in electrical stresses produced by sine and square wave voltages which result in significant differences in PD characteristics and motor winding insulation life. Therefore, it is essential to investigate the partial discharge (PD) behavior of inverter-fed motor insulation under square voltages [19], since the findings can have a significant impact on the design of the machine insulation system [20]. The results of PDIV tests may be used to assess the insulation system and, as a consequence, enhance the design of the motor winding insulation.

When applying impulse voltage, the choice of voltage waveform parameters can have a significant influence on PD and lifespan, resulting in varied outputs in the same insulating system [21]. Wang *et al.* [22] investigated the effect of repeated square voltage frequency on PD characteristics using turn-to-turn insulation models and observed that higher square voltage frequencies lead to fewer PD events and a lower average magnitude. Wang *et al*. [23] found a substantial difference in the PD amplitude, patterns, and frequency energy distribution between square wave voltages with a rise time of 100 to 200 ns and sinusoidal voltages with the same peak-to-peak and frequency. Montanari *et al.* [24] investigated PD properties of inverter-fed motor insulation systems that were tested with repeating square voltage. The results showed that a greater square voltage frequency could reduce PD occurrences with smaller magnitudes and shorter decay durations. It is also suggested that a square voltage of 50% duty cycle is probably the best choice for certifying and testing low-voltage inverter-fed rotating machines. Because dv/dt has an impact on the amplitude of PD, insulation lifespan at sinusoidal and square wave voltages with the same peak-to-peak voltage and frequency showed notable variances [25]. Under various temperature conditions, Wang *et al.* [26] examined the PD characteristics of a square waveform at 50 Hz with a peak-to-peak voltage of 2.5 kV. According to their findings, the impact of temperature on PD magnitude and delay duration is greater at lower frequencies, with higher temperatures producing PD events with greater magnitudes and longer delay times. Studies report that at 10–30 kHz, square-rising and square-spike waveforms show lifetimes with steep then declining slopes, while the square waveform degrades insulation more rapidly [27]. Sarathi *et al*. [28] conducted phase-resolved partial discharge analysis and observed that with increasing applied voltage, discharges occur during the rising portion of the waveform. Rapid voltage rise leads to visible surface discharges, which are more pronounced in the positive half cycle of AC voltage than in the negative half cycle. Additionally, asymmetrical AC voltages generate both high and low amplitude discharges. According to the researchers, the failure of twisted pair insulation is caused by the partial discharge being initiated by a high repetition frequency [29]. It has also been noted that while using the COMSOL software, PD appears in the micro gap between the twists.

The majority of reported experimental results were obtained under sinusoidal voltage circumstances [30], whereas only a small number of research have investigated the effect of square voltages on PD statistical properties, as mentioned in the existing literature. In this work, an attempt is made to assess the lifetime of twisted-pair enamel insulation by evaluating its PD characteristics under square voltages in the frequency range of 50 Hz to 5 kHz at room temperature, along with PDIV measurements at temperatures of 30 °C, 60 °C, and

90 °C. In the present experiment, twisted-pair polyester enamel samples are subjected to square and sine waveforms at frequencies ranging from 50 Hz to 5 kHz. The experimental results revealed significant variations in the PD statistical characteristics under square and sine voltages at different frequencies. The results indicate that the twisted-pair insulation system deteriorates more quickly under square waveform stress than under sine waveform stress. COMSOL is used to model the field distribution at a 0 mm air-gap length between twists, with an enamel thickness of 40 µm, at switching frequencies ranging from 50 Hz to 5 kHz. The simulations reveal that although square and sinusoidal voltages share the same peak-to-peak voltage and frequency, the square waveform generates higher electric field values, thereby raising the PD inception voltage between the gaps. The paper is organized into experimental setup and PD testing in section 2, results with high-frequency modeling (section 3), and analysis of PD amplitude and insulation degradation (section 4).

2. METHOD

2.1. Sample preparation

The twisted-pair samples are prepared using two enameled magnet wires twisted together in accordance with ASTM D1676-03 standards. A 40 µm thickness of single-coated polyester enamel insulation is employed for testing. The twisted-pair length is maintained at (12 ± 6) cm as per standard. The number of twists is 6 depending on the diameter the wire.

2.2. PD measurement setup

Figure 1 shows the partial discharge test setup. The sinusoidal AC supply voltage and square waveform with (50% duty cycle) different frequencies are simulated using a function generator (Tektronix, Model No AFG3051C) and signaled through a Trek amplifier (Model No 20/20C with 4 kV amplification factor). The partial discharge activity is then detected using a UHF sensor operating in the 300–3000 MHz frequency range after it has been supplied into the twisted pair [28] placed 20 cm distant from the twisted pair sample. A digital storage oscilloscope is attached to the output of the UHF sensor. The spectrum analyzer was set to zero-span mode for the resolved partial discharge experiments to understand the phase of occurrence of discharges with different frequencies of the sinusoidal and square waveforms as per the IEC 60270 standard [31].

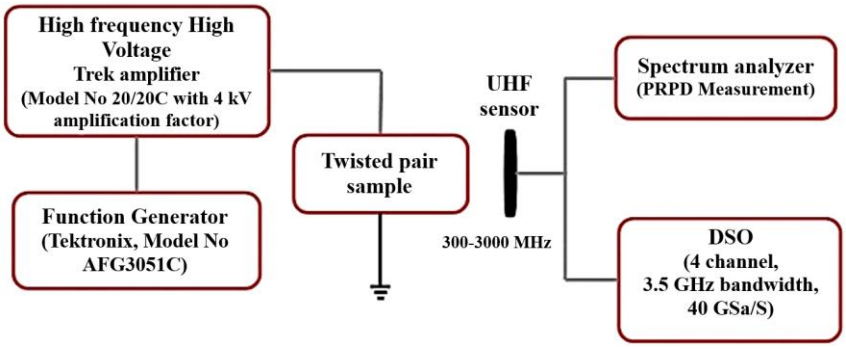

Figure 1. Schematic experimental setup for partial discharge studies

The PDIV and PD characteristic tests were conducted on twisted-pair specimens by applying the test voltage to the edge of one wire while grounding the edge of the other, thereby subjecting the enamel layers on both wires to high-voltage stress. The IEC 60270 standard was used to conduct the partial discharge investigations [31]. To conduct the PDIV test, the test voltage is progressively increased from a low level in order to determine the lowest voltage at which partial discharges take place. The test specimen is placed inside a temperature-controlled environmental chamber. PD measurements done at higher temperatures (e.g., 30 °C, 60 °C, 90 °C), high-frequency, high-voltage sine and square waveforms ranging from 50 Hz to 5 kHz were used to measure the PDIV and PRPD characteristics on insulation with enamel at room temperature ranging from 50 Hz to 5 kHz. The PD characteristics and PDIV were determined using the average results from five samples. Table 1 shows the PD test setup parameters along with the specifications of the sine and square waveforms.

Table 1. Details of the test setup

Frequency	Duty cycle	Waveforms and rise time	Test operating voltage
50 Hz, 1, 2.4, and 5 kHz	0-50%	Sine, Square (<1 µs)	0-20 kV (RMS)

3. RESULTS AND DISCUSSION

3.1. PDIV measurements at room temperature

The PDIV of twisted pair insulation was measured at room temperature using high-frequency sinusoidal and square voltage stresses. Figure 2 shows a histogram of average PD amplitude values for sine and square waveforms at various frequencies ranging from 50 Hz to 5 kHz. It is seen from the graphs that the corona inception voltage CIV (kV) increases with an increase in the frequency of both sine wave and square waveform as the polarization process dominates over the retention effect, leading to a higher PD magnitude at higher frequencies, similar to the trend reported in [32]. Additionally, the graphs indicate that PD inception for the square waveform occurs at a lower voltage than for the sine waveform across all frequencies. As a result, the square waveform consistently has a lower PDIV than the sine waveform. This implies that the insulation system of twisted pairs degrades more rapidly under square waveform stress, subjecting the insulation to more severe electrical stress compared to sine waveforms, which aligns with the results reported in [23].

3.2. PDIV measurements at higher temperatures

Twisted-pair insulation's PDIV was measured at 30 °C, 60 °C, and 90 °C while subjected to high-frequency sinusoidal and square voltage stress. Figures 3(a) and 3(b) show a histogram of average PD amplitude values for sine and square waveforms, respectively at higher temperatures over frequencies from 50 Hz to 5 kHz. At higher temperatures, PDIV decreases at all frequencies compared to room temperature. This is undesirable for motor winding insulation stressed at high temperatures under loaded conditions. The adverse effect of low PDIV at high temperatures is that it enhances the PD activity, uneven space charge accumulation and enhanced electrical aging processes, thus reducing the material lifetime and insulation reliability [33]. Furthermore, the graphs indicate that at higher frequencies, PDIV increases across all temperatures because the polarization process dominates over the retention effect [32]. Moreover, the graphs reveal that the corona inception voltage CIV (kV) decreases with increasing ambient temperature for both sine wave and square waveforms. The PD inception of the square waveform occurs at a lower voltage than that of the sine waveform at all frequencies and temperatures. Furthermore, at the same temperature and frequency, the PDIV of the square waveform is much lower than that of the sine waveform. As a result, as the temperature rises, the twisted-pair insulating system degrades more quickly under a square waveform than under a sine waveform. Hence, it is concluded at higher temperatures and higher frequencies, the PDIV of the square waveform is found to be detrimental to insulation compared to the designed stress of power frequency sine wave [34].

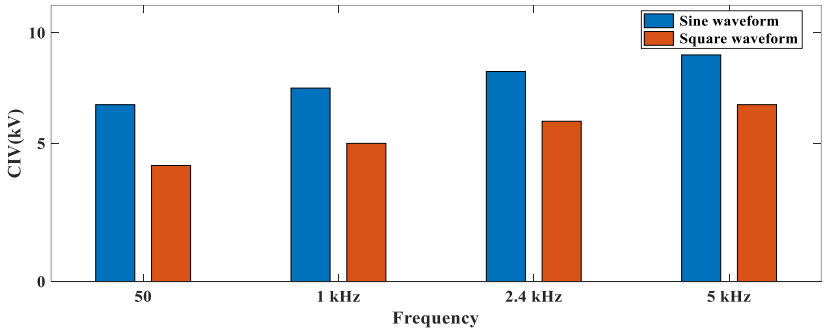

Figure 2. PDIV at 50 Hz, 1 kHz, 2.4 kHz, and 5 kHz under sine and square waveforms

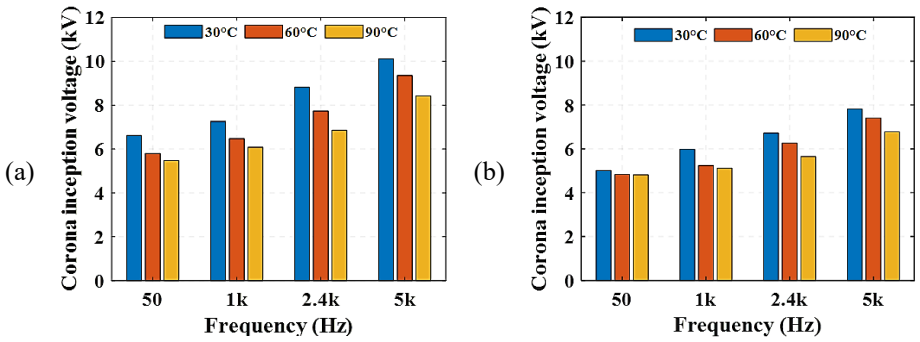

Figure 3. PDIV of (a) sine waveform and (b) square waveform at different temperatures

3.3. Sine and square waveforms PD characteristics at various frequencies

PD statistics are obtained by recording 600 cycles of data from PD pulses during the test. Figures 4 and 5 show the PRPD patterns of sine and square waveforms obtained from PD tests at different frequency levels, respectively. Figures 4(a)-4(d) show that at all frequencies, the discharges occur mostly in the rising part. For 50 Hz frequency, PD with a large magnitude occurs around 4 ms during the rising part, as shown in Figure 4(a). The amplitude increases from 20 a.u. to 50 a.u. at 1 kHz during the initial interval from 0 to 0.24 ms, as shown in Figure 4(b). At 2.4 kHz, it remains nearly constant, as illustrated in Figure 4(c), and then decreases to about 10 a.u. at 5 kHz, as shown in Figure 4(d). This behavior occurs because the polarization effect of space charge no longer dominates the variation of PD, while also influencing the degree of polarization and the diffusion process at higher frequencies [35]. However, for square wave stress, the discharge occurs throughout the cycle for 50 Hz and 1 kHz, but shifts towards a positive cycle as the frequencies increase to 2.4 kHz, and 5 kHz as shown in Figures 5(a)-5(d). The decrease in PD occurrence time and magnitude with rising frequency is consistent with the observations reported in [35]. Figure 5(a) shows that at 50 Hz frequency, PD with a small magnitude occurs from 0 to 20 ms throughout the cycle. The lesser magnitude PD is uniformly distributed from 0 to 1 ms for 1 kHz, as shown in Figure 5(b). At a frequency of 2.4 kHz, the PD activity is observed to be very intense, spread over a positive half cycle while the magnitude of PD pulses increased to about 30 a.u. as shown in Figure 5(c), similar to the trend reported in [36]. When the frequency is increased to 5 kHz, almost a similar effect is observed except that magnitude of PD pulses is increased from 10 a.u. to 25 a.u. as shown in Figure 5(d). Summarizing early PDIV at high temperature, at the square waveform, and high frequency, discussed in section 3.2 and PD characteristics discussed in section 3.3, the high-magnitude PD pulse at high frequency, stressed under a square waveform at high temperature, is found to be highly detrimental to insulating life, leading to premature failure. The results may help in estimating the lifespan of the insulation system and in designing new insulation systems capable of operating at high frequencies and high temperatures for various waveforms experienced by twisted pair rotating machine insulation. Hence, a new type of insulation (polymer nano composites) that can withstand such PWM stresses needs to be introduced and that should be higher dielectric strength and resistance to surface erosion is necessary. Investigating PD characteristics and insulation aging mechanisms under sine and square waveforms is crucial for ensuring reliable operation of inverter-fed drives in applications such as aircraft, electric vehicles (EVs), and renewable energy systems. Proactive design strategies, combined with careful material selection, can help prevent premature insulation failures. As a future direction, the influence of fast voltage rise times on PD inception in polymer insulation is proposed for investigation.

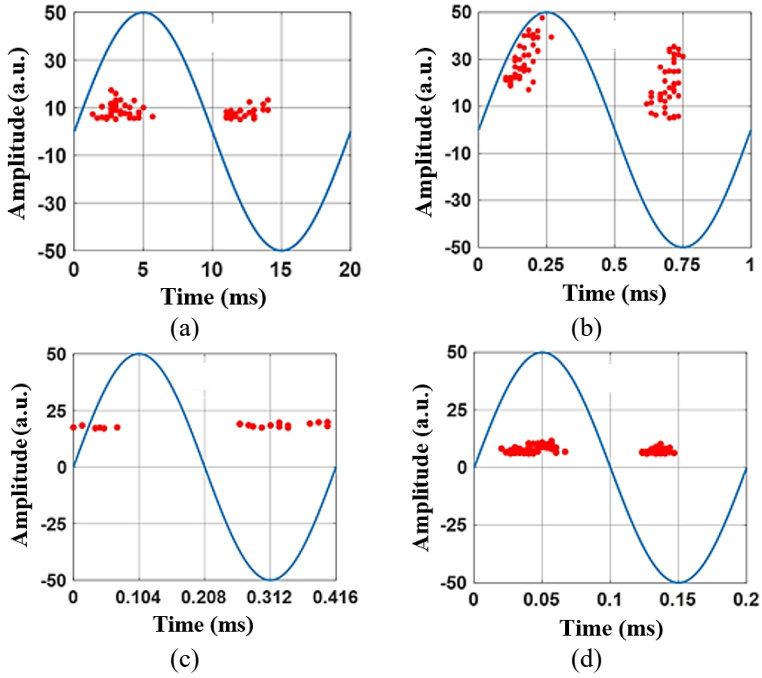

Figure 4. PRPD patterns of sine waveforms at (a) 50 Hz, (b) 1 kHz, (c) 2.4 kHz, and (d) 5 kHz

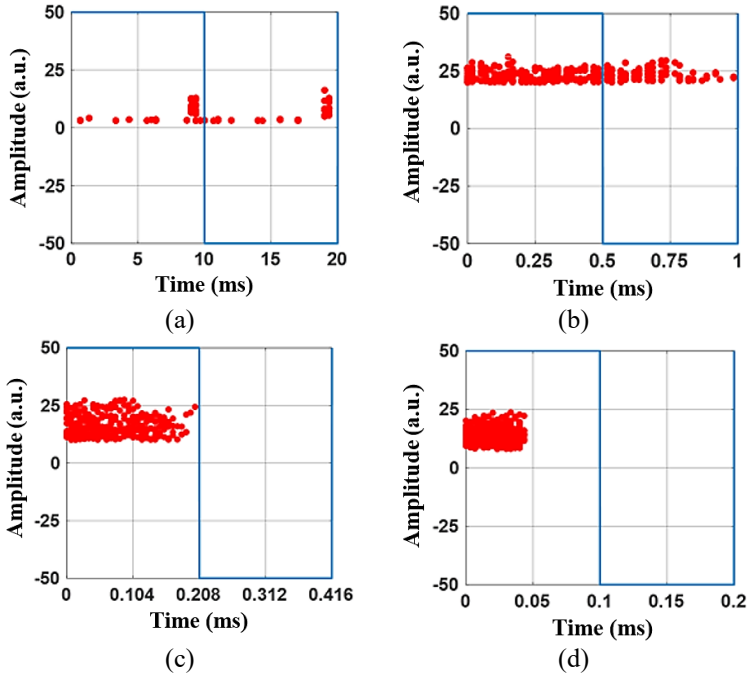

Figure 5. PRPD patterns of square waveforms at (a) 50 Hz, (b) 1 kHz, (c) 2.4 kHz, and (d) 5 kHz

3.4. High-frequency simulation of electric field distribution

3.4.1. Simulation parameters

A geometrically simplified model of winding wires without twists in the form of two conductors in direct contact (g = 0 mm) is investigated. The purpose of simulation in this work is to understand the stress experienced by twisted pairs, the contact points in particular. The COMSOL application was used to model the electric fields of two adjacent wires. The dielectric constant was taken as 3.3 and the polyester enamel thickness was 40 µm. The simulation was conducted using the following parameters: an enamel insulation thickness of 40 µm (0.04 mm), a copper conductor diameter of 0.72 mm (radius: 0.36 mm), and a surrounding rectangular boundary area of 1.9 mm². In the model, the left side of the inner layer of the two copper wires was assigned a high-voltage potential, while the right side was connected to ground. The simulation is configured using the AC/DC physics interface together with the heat transfer module. The electric currents model is employed to represent the electrical behavior, while heat transfer in solids is used to analyze the system's thermal effects. And mesh size is 0.121 mm. Table 2 lists the materials used in the simulation of the 2D electric field distribution.

Table 2. Properties of materials used for simulation

Material	ϵ_r, relative permittivity	σ, electrical conductivity [S/m]
Copper	1	5.998×10^{7}
Air	1	10^{-14}
Polyester	1.3	10^{-6}

Table 3 shows the sine and square waveform breakdown voltages between 50 Hz and 5 kHz. According to the table, the square wave has a lower breakdown voltage than the sine waveform at all frequencies. Furthermore, at 5 kHz, the square waveform reduced the breakdown voltage by 16.6 percent less than the sine wave. The cause of the reduced breakdown voltage at higher switching frequencies is discussed in [27]. Table 4 shows the simulation electric field values of sine and square waveforms. The table indicates that the electric field value in the simulation rises at a frequency of 5 kHz. This is due to the application of heat physics in simulation, which causes dielectric losses to impact the computation. This is due to the usage of heat physics in the simulation incorporates the dielectric losses as a heat input. This further affects temperature distribution and thus electric field will increase. As a result, it is found that a lesser reduction in breakdown voltage results in higher electric stress at 5 kHz frequency is reported in [37]. The applied voltage was considered as the breakdown voltage for the sine waveform in simulation for all frequencies. Figure 6 shows the electric field distribution of two parallel conductors in direct contact between them.

Table 3. The breakdown voltage of sine and square waveforms

Frequency	Breakdown voltage of sine wave (kV_{rms})	Breakdown voltage of square wave (kV_{rms})
50 Hz	8	5.8
1 kHz	8.6	6.6
2.4 kHz	9	7.4
5 kHz	9.6	8

Table 4. Simulation electric field values (kV/mm) for sine and square waveforms

Frequency	Sine waveform	Square waveform
50 Hz	260	265
1 kHz	283	287
2.4 kHz	286	296
5 kHz	290	316

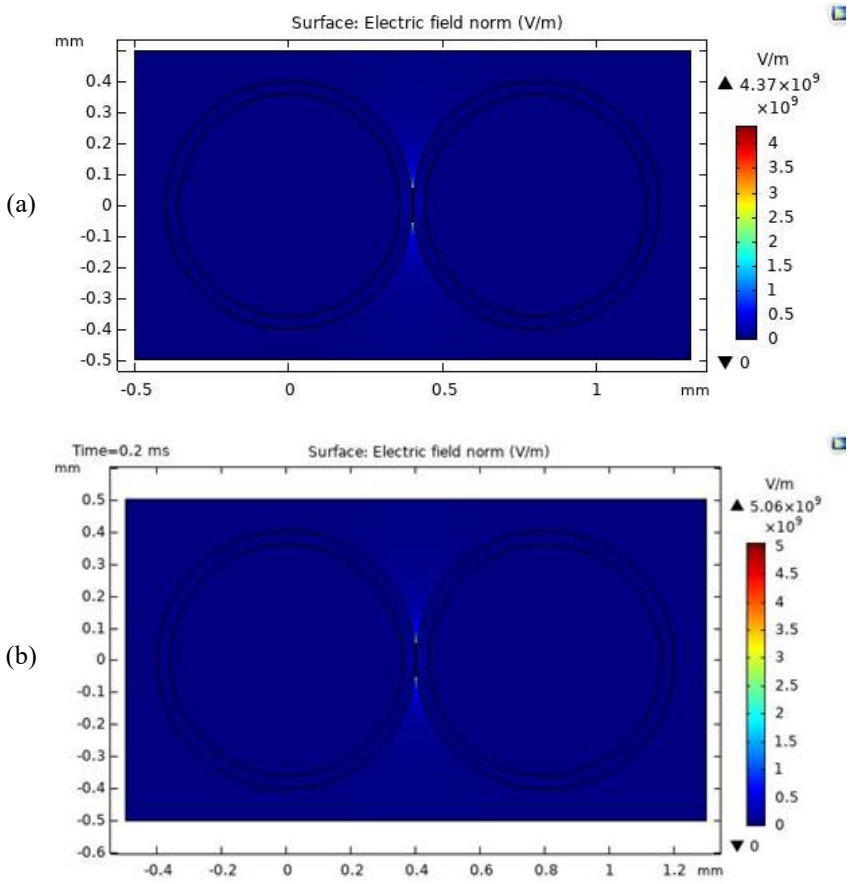

Figure 6. The 2D electric field distribution at 5 kHz with an air gap of 0 mm: (a) sine waveform and (b) square waveform

The electric field is observed to be the highest on the wire insulation surface at the wire contact point. Figure 7 shows how the electric field distribution differs for sine and square waveforms. The graph indicates the maximum electric field at 5 kHz, with smaller fields at 50 Hz, 1 kHz, and 2.4 kHz for sine and square waveforms. At all these frequencies, the square waveform exhibits a higher electric field strength than the sine waveform. Because of air gap ionization and surface potential decay [27], the electric field on the wire insulation surface remains sufficiently high to initiate PD under both waveforms. A higher square waveform electric field value leads to a higher PDIV as compared to a sine waveform of the same applied voltage and frequency, consistent with the trends reported in [23], [25]. This shows how high frequency affects the electric field distribution in the air gap between the wires and on their surfaces. Moreover, PD generated by high frequency stress, which increases the PD inception voltage level, leads to insulation failure. Therefore, new insulation materials and design approaches are needed for low-voltage motor insulation to ensure greater PD resistance at higher operating frequencies.

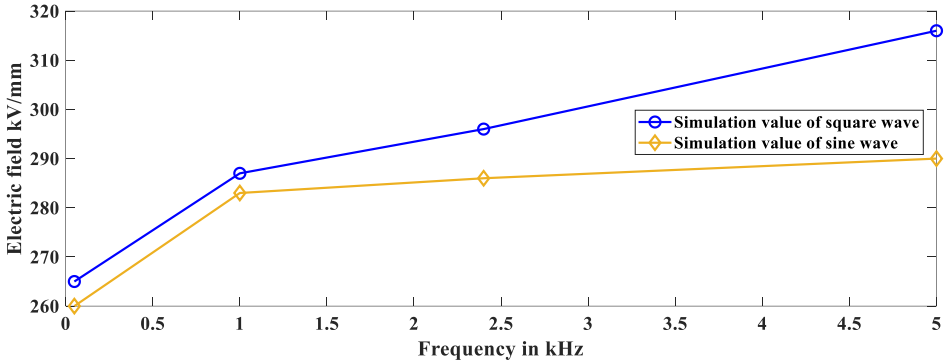

Figure 7. Electric field distribution of sine and square waveforms at different frequencies from 50 Hz to 5 kHz, with 0 mm air gap

4. CONCLUSION

High switching frequency is a major factor contributing to insulation reliability issues. At higher temperatures, PDIV decreases at all frequencies compared to room temperature. Furthermore, it can be seen from the graphs that the corona inception voltage CIV (kV) decreases with increasing ambient temperature for both sine wave and square waveforms. The PD inception of the square waveform occurs at a lower voltage than that of the sine waveform at all frequencies and temperatures. Hence, as the temperature increases, the degradation rate of the twisted pair insulation system using a square waveform is faster than that of the sine waveform. At lower frequencies up to 1 kHz, though the PD amplitude is high for sinusoidal waveform stress, the magnitude reduces at higher frequencies up to 5 kHz and the PD activity is less. However, when stressed under square waveform, intense PD activity is observed mainly over a positive half cycle pointing to the deleterious effect of square waveform stress at high frequency. As a result, the twisted pair insulation system degrades more rapidly under a square waveform than a sine waveform, indicating that converter operation subjects the insulation to higher electrical stress. From the simulation, the square waveform produces the highest electric field in the gap between the wires and on their surfaces, with lower values in other regions compared to the sine waveform. Furthermore, it is found that the square waveform has significant electric field stress in all the above-mentioned frequencies as compared to the sine waveform, which causes the early breakdown of the enamel insulation. At higher switching frequencies, the impact of partial discharges from square waveforms on enamel insulation becomes so severe that the twisted-pair samples fail prematurely. Therefore, further research is needed to develop magnetic wires with high PD resistance for low-voltage motors operating at higher operating frequencies.

FUNDING INFORMATION

The authors declare that no funding was received for this research.

AUTHOR CONTRIBUTIONS STATEMENT

This journal uses the Contributor Roles Taxonomy (CRediT) to recognize individual author contributions, reduce authorship disputes, and facilitate collaboration.

Name of Author	C	M	So	Va	Fo	I	R	D	O	E	Vi	Su	P	Fu
S. Narasimha Rao	✓	✓	✓		✓		✓	✓	✓	✓				
Elanseralathan Kasinathan	✓	✓	✓	✓	✓	✓			✓	✓	✓	✓	✓	
Ramanujam Sarathi				✓	✓	✓	✓	✓		✓	✓	✓	✓	

C : **C**onceptualization
M : **M**ethodology
So : **So**ftware
Va : **Va**lidation
Fo : **Fo**rmal analysis
I : **I**nvestigation
R : **R**esources
D : **D**ata Curation
O : Writing - **O**riginal Draft
E : Writing - Review & **E**diting
Vi : **Vi**sualization
Su : **Su**pervision
P : **P**roject administration
Fu : **Fu**nding acquisition

CONFLICT OF INTEREST STATEMENT

Authors state no conflict of interest.

DATA AVAILABILITY

Data availability is not applicable to this paper.

REFERENCES

[1] P. Wang, C. Zheng, Y. Li, Y. Lei, A. Cavallini, "The PD and endurance features of enameled wires at short repetitive impulsive voltages," *IEEE Electrical Insulation Conference EIC,* pp. 572-576, June 2018, doi: 10.1109/EIC.2018.8481043.

[2] V. N. Höpner, V. E. Wihelm, "Insulation life span of low voltage electric motors-a survey," *Journal of Energies*, vol. 14, pp .1-32, March 2021, doi:1996-1073/14/6/1738.

[3] M. Florkowski, "Magnetic field effects on partial discharges in electrical insulation subjected to PWM excitation," *IEEE Transactions on Power Electronics*, vol. 39, no. 2, pp. 2741-2750, Feb. 2024, doi: 10.1109/TPEL.2023.3334011.

[4] Lusuardi, A. Cavallini, M. G. de la Calle, J. M. Martínez-Tarifa, G. Robles, "Insulation design of low voltage electrical motors fed by PWM inverters," *IEEE Electrical Insulation Magazine*, vol. 35, no. 3, pp. 7-15, June 2019, doi: 10.1109/MEI.2019.8689431

[5] Y. Xie, J. Zhang, F. Leonardi, A. R. Munoz, M. W. Degner, F. Liang, "Voltage stress modeling and measurement for random-wound windings driven by inverters," *IEEE International Electric Machines & Drives Conference (IEMDC)*, August 2020, pp 1917-1924, doi: 10.1109/TIA.2020.2986184.

[6] R. Leuzzi, V. G. Monopoli, F. Cupertino, P. Zanchetta, "Active ageing control of winding insulation in high frequency electric drives," *IEEE Energy Conversion Congress and Exposition (ECCE),* 2018, pp. 1-7, doi: 10.1109/ECCE.2018.8558257

[7] Z. Wei, H. You, B. Hu, R. Na, J. Wang, "Partial discharge behavior on twisted pair under ultra-short rise time square-wave excitations," *IEEE Electrical Insulation Conference EIC,* 2019, pp. 493-496, doi: 10.1109/EIC43217.2019.9046624.

[8] A. Caprara and G. Ciotti, "Investigation about the effect of the voltage profile on RPDIV and time to failure for insulation materials subjected to impulsive stress conditions," *IEEE Electrical Insulation Conference (EIC)*, 2022, pp. 98-101, doi: 10.1109/EIC51169.2022.9833191.

[9] L. Lusardi *et al.,* "The effect of inverter characteristics on partial discharge and life behavior of wire insulation," *IEEE Electrical Insulation Magazine*, vol. 34, no. 2, pp. 32-39, April 2018, doi: 10.1109/MEI.2018.8300442.

[10] F. Guastavino, E. Torello, L. D. Giovanna, and I. Khan, "Study of the partial discharge inception voltage variation over time on enameled wires subjected to thermal-electrical stress," *IEEE Conference on Electrical Insulation and Dielectric Phenomena (CEIDP)*, 2023, pp. 1-3, doi: 10.1109/CEIDP51414.2023.10410540.

[11] M. Kozako *et al.*, "Prediction of lifetime in surge resistant enamel twisted pair by partial discharge degradation under repetitive impulse voltage application," *IEEE 4th International Conference on Dielectrics (ICD)*, 2022, pp. 261-264, doi: 10.1109/ICD53806.2022.9863577.

[12] Rotating Electrical Machines—Part 18-41: Partial discharge free electrical insulation systems (Type I) used in rotating electrical machines fed from voltage converters—qualification and quality control tests, document, *IEC 60034-18-41*, 2014.

[13] Rotating Electrical Machines—Part 18-42: Qualification and acceptance tests for partial discharge resistant electrical insulation systems (Type II) used in rotating electrical machines fed from voltage converters, document, *IEC 60034-18-42*, 2016.

[14] F. Guastavino, F. Rossi, C. Gianoglio, E. Torello and D. Cordano, "PDIV and RPDIV on different temperatures on different kind of type I insulating system," *IEEE Conference on Electrical Insulation and Dielectric Phenomenon (CEIDP*), 2017, pp. 369-372, doi: 10.1109/CEIDP.2017.8257591.

[15] S. Matsumoto, N. N. Nam, D. Nagaba, and T. Ogiya, "Partial discharge characteristics of twisted magnet wire under high frequency AC voltage," *International Symposium on Electrical Insulating Materials*, 2014, pp. 57-60, doi: 10.1109/ISEIM.2014.6870719.

[16] P. Seri and G. C. Montanari, "A voltage threshold in operating condition of PWM inverters and its impact on reliability of insulation systems in electrified transport applications," *IEEE Transactions on Transportation Electrification*, vol. 7, no. 1, pp. 69-77, March 2021, doi: 10.1109/TTE.2019.2957605.

[17] S. Ma, P. Wang, and Y. Zhu, "A novel PD detection method for inverter-fed motor using shell as slot antenna," *International Conference on Electrical Materials and Power Equipment,* pp. 1-4, 2023, doi: 10.1109/ICEMPE57831.2023.10139470.

[18] S. S. Vala, A. B. Mirza, and F. Luo, "A review on partial discharge phenomenon in rotating machines operated using WBG motor drives," *IEEE Transportation Electrification Conference & Expo (ITEC),* pp. 523-528, 2022, doi: 10.1109/ITEC53557.2022.9814056.

[19] K. Hameyer, A. Ruf, F. Pauli, "Influence of fast switching semiconductors on the winding insulation system of electrical machines," *International Power Electronics Conference, (IPEC)*, pp. 740-745, 2018, doi: 10.23919/IPEC.2018.8507972.

[20] Y. Zhao, G. Zhang, R. Guo and F. Yang, "The breakdown characteristics of thermostable insulation materials under high-frequency square waveform," *IEEE Transactions on Dielectrics and Electrical Insulation*, vol. 26, no. 4, pp. 1073-1080, August 2019, doi: 10.1109/TDEI.2019.007856.

[21] F. Guastavino and A. Dardano, "Life tests on twisted pairs in presence of partial discharges: influence of the voltage waveform," *IEEE Transactions on Dielectrics and Electrical Insulation*, vol. 19, no. 1, pp. 45–52, Feb. 2012, doi: 10.1109/TDEI.2012.6148501.

[22] P. Wang, A. Cavallini and G. C. Montanari, "The influence of impulsive voltage frequency on PD features in turn insulation of inverter-fed motors," *IEEE Conference on Electrical Insulation and Dielectric Phenomena (CEIDP*), pp. 35-38, 2014, doi: 10.1109/CEIDP.2014.6995876.

[23] P. Wang, J. Wang, H. Xu, K. Zhou, Y. Lei, and Q. Zhou, "Comparative study of PD characteristics for inverter-fed motor insulation under sinusoidal and repetitive square wave voltage conditions," *IEEE International Conference on High Voltage Engineering and Application (ICHVE)*, pp. 1-4, 2016, doi: 10.1109/ICHVE.2016.7800806.

[24] G. C. Montanari, P. Seri and R. Hebner, "Type of supply waveform, partial discharge behavior and life of rotating machine insulation systems," *IEEE International Power Modulator and High Voltage Conference (IPMHVC)*, pp. 176-179, 2018, doi: 10.1109/IPMHVC.2018.8936775.

[25] P. Wang, M. Zhao, Q. Zhou, and J. Zhang, "The influence of SPWM frequency on the endurance of inverter-fed motor insulation," *IEEE Conference on Electrical Insulation and Dielectric Phenomena (CEIDP)*, pp. 142-145, 2019, doi: 10.1109/CEIDP47102.2019.9009763.

[26] P. Wang, H. Xu, J. Wang, A. Cavallini, and G. C. Montanari, "Temperature effects on PD statistics and endurance of inverter-fed motor insulation under repetitive square wave voltages," IEEE *Electrical Insulation Conference (EIC),* pp. 202-205, 2016, doi: 10.1109/EIC.2016.7548695.
[27] S. N. Rao and K. Elanseralathan, "Modeling of high frequency high voltage of waveforms on the life of enamel insulation," *Indonesian Journal of Electrical Engineering and Computer Science (IJEECS)*, vol. 23, no. 3, Sep. 2021, pp. 1331-1339, doi: 10.11591/iijeecs. v23.i. pp1331-1339.
[28] R. Sarathi, I. P. Merin Sheema, J. Sundara Rajan, and M. G. Danikas, "Influence of harmonic AC voltage on surface discharge formation in transformer insulation," *IEEE Transactions on Dielectrics and Electrical Insulation*, vol. 21, no. 5, pp. 2383-2393, Oct. 2014, doi: 10.1109/TDEI.2014.004448.
[29] M. Florkowski, B. Florkowska, and P. Zydron, "Partial discharges in insulating systems of low voltage electric motors fed by power electronics-twisted-pair samples evaluation," *Journal of Energies*, vol. 12, no. 5, pp. 1-19, 2019, doi: 10.3390/en12050768.
[30] P. Wang, "Effect of repetitive square voltage frequency on PD features," *Science China Technological Sciences*, vol. 56, no. 1, pp. 1313-1321, February 2013, doi: 10.1109/TDEI.2013.6451364.
[31] High-voltage test techniques - partial discharge measurements, *IEC 60270 International Standard*, Rev. 3, December 2000
[32] J. Jiang, B. Zhang, Z. Li, P. Ranjan, J. Chen and C. Zhang, "Partial discharge features for power electronic transformers under high-frequency pulse voltage," *IEEE Transactions on Plasma Science*, vol. 49, no. 2, pp. 845-853, Feb. 2021, doi: 10.1109/TPS.2021.3053960.
[33] Y. Ji, P. Giangrande, and W. Zhao, "Effect of environmental and operating conditions on partial discharge activity in electrical machine insulation: a comprehensive review," *Energies*, vol. 17, no. 16, p. 3980, Aug. 2024, doi: 10.3390/en17163980.
[34] B. Zhang, J. Jiang, Z. Li, X. Li, P. Ranjan, and C. Zhang, "Partial discharge analysis of power electronic transformers under high frequency pulse voltage," *International Symposium on High Voltage Engineering (ISH 2021)*, 2021, pp. 1872-1876, doi: 10.1049/icp.2022.0182.
[35] Jun Jiang *et al*., "Partial discharge analysis in high-frequency transformer based on high-frequency current transducer" *Journal of energies*, vol. 11, no. 5, pp. 1-13, Jul. 2018, doi: 10.3390/en11081997.
[36] P. Wang *et al.,* "Effect of repetitive impulsive and square wave voltage frequency on partial discharge features," *International Conference on the Properties and Applications of Dielectric Materials (ICPADM)*, pp. 152-155, 2018, doi: 10.1109/ICPADM.2018.8401153.
[37] W. Wang *et al*., "Electric stress and dielectric breakdown characteristics under high-frequency voltages with multi-harmonics in a solid-state transformer," *International Journal of Electrical Power and Energy Systems*, vol 129, pp.1-9, July 2021, doi: 10.1016/j.ijepes.2021.106861.

BIOGRAPHIES OF AUTHORS

Dr. S Narasimha Rao received his B.Tech. degree from S.V. College of Engineering, S.V. University in 2004, and M.E. degree from Sathyabama University, Chennai, India in 2010, and Ph.D. degree from Pondicherry Central University, Puducherry, India in the year 2023. He is currently working as an associate professor in the Department of EEE, Siddharth Institute of Engineering & Technology, Puttur, Andhra Pradesh, India. His areas of interest are partial discharge, motor winding insulation, and modeling of insulation. He can be contacted at email: snrinskit@ptuniv.edu.in.

Dr. Elanseralathan Kasinathan received his B.Tech. degree from Mahatma Gandhi University, Kottayam in 1992, and M.E. degree from the Indian Institute of Science, Bangalore, India in 1999, and his Ph.D. degree from the Indian Institute of Technology Kanpur, India in the year 2009. He is currently working as a professor in the Department of EEE, Puducherry Technological University, Puducherry, India. His areas of interest are partial discharge, modeling of insulation, nano dielectrics, and energy storage. He can be contacted at email: pecelan@ptuniv.edu.in.

Dr. Ramanujam Sarathi is currently a professor and head of the High Voltage Laboratory, Department of Electrical Engineering, IIT Madras, Chennai, India. He obtained his Ph.D. degree from the Indian Institute of Science, Bangalore, in 1994. His research area includes condition monitoring of power apparatus and nanomaterials. He can be contacted at email: sarathi@ee.iitm.ac.in.